

## THREE-DIMENSIONAL ANALYSIS FOR FUEL PIN DEFORMATIONS IN AN LMFBR ASSEMBLY

K. MIKI

*Atomic Energy Research Laboratory, Hitachi Ltd.,  
Ozenji, Tama-ku, Kawasaki, Kanagawa, 215, Japan*

### SUMMARY

A new analytical method is presented for analyzing, in three dimensions, the mechanical response of fuel pins with wire spacers, to their thermal and neutronic environment in an assembly of a Liquid Metal cooled Fast Breeder Reactor (LMFBR). It analyzes the mechanical interactions of the fuel pins in the assembly corresponding to three directions, which form an angle of  $\pi/3$  radians with one another, and is based on the mathematical relationship of the displacements at the contact points and the associated contact forces with respect to all fuel pins in a direction corresponding to one of three axes. The displacement of the fuel pin is composed of its three components in each of the three directions thus calculated. In particular this method makes it possible to take into precise consideration the two factors affecting the deformation of the fuel pins—(a) the mutual interaction of fuel pins and (b) the forced bending of the fuel pins due to the deformation of the wrapper tube.

Based on this method, a new computational code, the Subchannel Deformation Analysis Code for Wire-Wrapped Assemblies (SHADOW), has been developed, which can be applied to seven kinds of wire-wrapped fuel assemblies with a number of fuel pins ranging from 7 to 169. This code calculates subchannel flow areas, wetted perimeters, gaps between fuel pins and distances between the outermost pins and wrapper tube wall, coupled with a thermal hydraulic code in order to get the temperature distributions of coolant and cladding in the deformed flow channels. SHADOW also calculates the magnitudes, positions and directions of contact forces loaded by the adjacent fuel pins or wrapper tube.

SHADOW was utilized for analyzing the deformation due to thermal bowing of 169 fuel pins in a prototype fast breeder reactor. Conclusions derived from the present study are summarized as follows:

- (1) The bowing deformations are significant throughout the overall length of the outer fuel pins and in the upper part of the gas plenum region of the inner fuel pins. These phenomena cause the axial variations of the flow areas, especially, in the outer channels and requires iterative estimations of the temperature distribution in the deformed channels.
- (2) In the case of the outer fuel pins, the major contact forces are loaded near the top of each fuel pin, and in the case of the inner ones, the loads are mainly applied near the center parts of the gas plenum and core regions. These forces are not large enough to deform the cross section of the cladding. The computational time in the present study is less than 20 minutes on the IBM 370/158. It was confirmed that SHADOW is an effective tool for analyzing or evaluating the thermal and structural designs of LMFBR fuel assemblies of the wire-wrapped-type.

## 1. Introduction

In thermal-hydraulic design of a Liquid Metal cooled Fast Breeder Reactor (LMFBR), the maximum operation temperature of the cladding should be kept below the predetermined limiting value, while the cladding temperature is extremely sensitive to that of the coolant flowing in the fuel assembly. It is, therefore, required to accurately estimate the coolant temperature during operation and, in particular, to analyze the deformation of coolant flow channels within the fuel assembly.

If coolant flow channels are deformed in the peripheral region of the assembly, the temperature of the wrapper tube wall deviates from its nominal value, which causes bowing deformation of the wrapper tube with the potential of a core deformation. Consequently, the deformation of coolant flow channels can give rise to some problems in other design fields of an LMFBR, such as large reactivity change in nuclear design, unexpected loads upon the core structures in structural design, and difficulty with control rod insertion and fuel assembly exchange.

In a grid-spaced fuel assembly, the fuel pin bundle is tightly clustered by grid spacers, and therefore deformation of fuel pins in the assembly can be treated easily under some appropriate assumptions. Hence, extensive work has been carried out [1-4] concerning the analysis of flow channel deformation in this type of fuel assemblies.

In a wire-wrap fuel assembly, on the other hand, the spacing of fuel pin support points depends on deformation of each fuel pin, since each fuel pin is fixed only at the lower end and the gap between the fuel pins is larger than the diameter of wire spacer at the time of manufacture. In order to analyze flow channel deformation, it is necessary to take into account the mechanical interactions among all fuel pins within the assembly.

The present paper proposes an analytical method for deformation of fuel pins in a wire-wrap fuel assembly. Based on this method, a new computational code, the Subchannel Deformation Analysis Code for Wire-Wrapped Assemblies (SHADOW), has been developed, which can be applied to seven kinds of hexagonal assemblies with the number of fuel pins ranging from 7 to 169. This code is applied to analyze the deformation due to thermal bowing of 169 fuel pins in an assembly of a prototype fast breeder reactor.

2. Analytical Method

2.1 Decomposition of Fuel Pin Displacement into Three Directions

In the present method the components of the displacement of fuel pins are calculated in three directions with an angle of  $\pi/3$  radians in between and then synthesized into an actual displacement. This way of approach is appropriate because of the triangular arrangement of fuel pins in an fuel assembly.

If the fuel pin is loaded by the contact forces from the adjacent fuel pins or wrapper tube as shown in Fig. 1, in addition to being affected by the bending moment due to thermal expansion and swelling, the components of its displacement are expressed as follows:

$$EI \frac{d^2 y_\phi}{dz^2} = - M_\phi(Z) + \sum_{\phi'} f_{\phi, \phi'} \cdot R_{\phi'} \cdot (l_{\phi'} - Z) \cdot U(l_{\phi'} - Z) + R_\phi \cdot (l_\phi - Z) \cdot U(l_\phi - Z), \quad (1)$$

$$(\phi' \neq \phi)$$

$$(\phi = 0, \frac{1}{3}\pi, \frac{2}{3}\pi),$$

- where  $\phi$  : direction of a row, denoting the angle from the reference direction,
- $y_\phi$  : component of displacement towards the  $\phi$  direction,
- $M_\phi$  : bending moment in the  $\phi - Z$  plane due to thermal expansion and swelling,
- $R_\phi$  : contact force in the  $\phi$  direction,
- $l_\phi$  : position of the contact point in the Z direction,
- $f_{\phi, \phi'}$  :  $\phi$  component of the unit contact force  $R_{\phi'}$ , which is given by

$$f_{\phi, \phi'} = \begin{cases} 1 & \text{for } \phi = \phi' \\ \pm \frac{1}{2} & \text{for } \phi \neq \phi' \end{cases},$$

$U(t)$  : unit step function defined by

$$U(t) = \begin{cases} 1 & \text{for } t \geq 0 \\ 0 & \text{for } t < 0 \end{cases}.$$

For the sake of simplicity, the number of contact points is assumed to be one in each direction.

If the displacement is decomposed into two directions making a right angle to each other, the two equations expressing the component of the displacement can be treated independently since  $f_{\phi, \phi'} = 0$  for  $\phi \neq \phi'$ . The present method, on the other hand, necessitates the simultaneous treatment of three equations given by eq.(1), since the contact forces in other two directions affect the component in the considered direction through the second term of the right hand side of eq.(1).

However, the three equations can be treated independently, making use of the following iterative procedure as an approximate method:

Step 1: Calculate the contact forces,  $R^{(1)}$ , between fuel pins in a row, neglecting the second term of the right hand side of eq. (1).

This calculation is repeated for all rows in each direction.

Step 2: Reevaluate the second guess  $R^{(2)}$  of the contact forces, by substituting  $R^{(1)}$  into the second term of the equation.

Step 3: Repeat the same procedure as in Step 2 using the contact forces obtained in the previous iteration.

In the above procedure, the solution will not diverge since the contact forces substituted into the second term are loaded in the opposite direction to the displacement of the fuel pin and  $f_{\phi, \phi'} = \pm \frac{1}{2}$  for  $\phi \neq \phi'$ .

## 2.2 Mechanical Interactions between Fuel Pins in a Row

### 2.2.1 Location of Contact Points between Fuel Pins

The procedure for locating contact points between fuel pins is based on the following view:

A contact point is located in the region where adjacent fuel pins overlap after deformation and the difference between the displacements of the pins reaches the maximum.

If fuel pins bow freely as the broken lines in Fig. 2, the axial heights of contact points are  $l_1$  and  $l_2$  between fuel pins 1 and 2, and  $l_3$  between fuel pins 2 and 3. Then, the contact forces can be obtained by means of the method described in the next section. And the forced bendings, calculated by the contact forces, are superimposed upon the free bowings, which leads to the solid lines of the fuel pin shapes shown in Fig. 2. Fuel pin 1 has, then, no contact with fuel pin 2 at the height  $l_2$  because of the contact at the height  $l_1$ . Furthermore, fuel pin 3 comes in contact with fuel pin 4 due to the interference between fuel pins 2 and 3. Taking into account these two phenomena, we propose the calculational scheme represented in Fig. 3 for locating the contact points. In the scheme the inner loop is provided for checking whether the clearance exists between fuel pins and the outer loop for finding a new contact point.

### 2.2.2 Derivation of Matrix Equation

Let  $l_k^i$  and  $R_k^i$  ( $k = 1, 2, \dots, m(i)$ ;  $i = 1, 2, \dots, n + 1$ ) be the axial heights of contact points and contact forces, respectively, as shown in Fig. 4, where  $m(i)$  is the total number of contact points between the  $(i-1)$ -th and the  $i$ -th fuel pins, and  $n$  is the total number of fuel pins in a row. In Fig. 4,  $t$  is a gap between fuel pins, whereas  $s$  denotes a gap between the outermost fuel pin and the wrapper tube wall. For the sake of simplicity, they are assumed to be constant over the axial length before deformation.

The displacement,  $y_i(Z)$ , of the  $i$ -th fuel pin at position  $Z$  can be divided into two parts

$$y_i(Z) = y_i^T(Z) + y_i^R(Z), \quad (i = 1, 2, \dots, n), \quad (2)$$



or, in brief,

$$\hat{A} \vec{R} = \vec{\phi} \quad , \quad (7)$$

where  $\hat{A}$  is a block-tridiagonal matrix, and the matrices  $A_1$ ,  $B_1$  and  $C_1$  are given by

$$A_1 = 2 \begin{bmatrix} g(\ell_1^1, \ell_1^1) & \text{-----} & g(\ell_{m(1)}^1, \ell_1^1) \\ & g(\ell_j^1, \ell_k^1) & \\ g(\ell_1^1, \ell_{m(1)}^1) & \text{-----} & g(\ell_{m(1)}^1, \ell_{m(1)}^1) \end{bmatrix} \quad , \quad (8)$$

$$B_1 = - \begin{bmatrix} g(\ell_1^{i-1}, \ell_1^i) & \text{-----} & g(\ell_{m(i-1)}^{i-1}, \ell_1^i) \\ & g(\ell_j^{i-1}, \ell_k^i) & \\ g(\ell_1^{i-1}, \ell_{m(i)}^i) & \text{-----} & g(\ell_{m(i-1)}^{i-1}, \ell_{m(i)}^i) \end{bmatrix} \quad , \quad (9)$$

$$C_1 = - \begin{bmatrix} g(\ell_1^{i+1}, \ell_1^i) & \text{-----} & g(\ell_{m(i+1)}^{i+1}, \ell_1^i) \\ & g(\ell_j^{i+1}, \ell_k^i) & \\ g(\ell_1^{i+1}, \ell_{m(i)}^i) & \text{-----} & g(\ell_{m(i+1)}^{i+1}, \ell_{m(i)}^i) \end{bmatrix} \quad , \quad (10)$$

and the vectors  $\vec{R}_1$  and  $\vec{\phi}_1$ , ( $i = 1, 2, \dots, n+1$ ) are given by

$$\vec{R}_1 = \begin{bmatrix} R_1^1 \\ R_2^1 \\ \vdots \\ R_{m(1)}^1 \end{bmatrix} \quad , \quad (11)$$

$$\vec{\phi}_1 = \begin{bmatrix} Y_1(\ell_1^1) - s - y^T(\ell_1^1) \\ Y_1(\ell_2^1) - s - y^T(\ell_2^1) \\ \vdots \\ Y_1(\ell_{m(1)}^1) - s - y^T(\ell_{m(1)}^1) \end{bmatrix} \quad , \quad (12)$$

$$\vec{\phi}_i = \begin{bmatrix} y_{i-1}^T(\ell_1^i) - t - y_i^T(\ell_1^i) \\ y_{i-1}^T(\ell_2^i) - t - y_i^T(\ell_2^i) \\ \vdots \\ y_{i-1}^T(\ell_{m(i)}^i) - t - y_i^T(\ell_{m(i)}^i) \end{bmatrix} \quad , \quad (i = 2, 3, \dots, n) \quad (13)$$

$$\vec{\phi}_{n+1} = \begin{bmatrix} y_n^T(\ell_1^{n+1}) - s - Y_2(\ell_1^{n+1}) \\ y_n^T(\ell_2^{n+1}) - s - Y_2(\ell_2^{n+1}) \\ \vdots \\ y_n^T(\ell_{m(n+1)}^{n+1}) - s - Y_2(\ell_{m(n+1)}^{n+1}) \end{bmatrix} \quad (14)$$

### 2.2.3 Properties of Matrix

The matrices  $A_1$ ,  $B_1$  and  $C_1$  have the following properties.

- (i)  $A_1$  is a symmetric matrix.
- (ii) The matrix  $B_{i+1}$  is equivalent to the transpose of the matrix  $C_i$ .

Consequently, the coefficient matrix  $\tilde{A}$  can be shown to be symmetric, and its order,  $M$ , is equal to the sum of the orders of the matrix  $A_1$ , i.e.,

$$M = \sum_{i=1}^{n+1} m(i) \quad (15)$$

In solving the matrix equation eq. (7), utilization of the two properties of the coefficient matrix  $\tilde{A}$  — block - tridiagonal and symmetric — makes it possible to reduce the calculation time to less than 1/100 and the computer storage capacity to less than 1/10 as compared with calculating directly the inverse matrix of  $\tilde{A}$ .

### 3. Description of SHADOW Code

A new computational code SHADOW has been developed based on the analytical method described in Chap. 2. Fig. 5 illustrates a calculation flow in SHADOW. Main input data provided to SHADOW are categorized into three groups; (1) displacements of a wrapper tube, (2) temperature distributions of the coolant and the cladding in a fuel assembly and (3) fast neutron flux distribution in an assembly. The first data are obtained through a core deformation analysis code, such as HICODEM [5], analyzing mechanical interactions between fuel assemblies and calculating deflections of them. The second data are given by a thermal-hydraulic analysis code, such as DIANA [6]. The third one is given by a nuclear analysis code, such as CITATION [7], in order to calculate swelling in fuel assembly components.

With these data the newly developed code SHADOW analyzes the mechanical response of fuel pins to their thermal and neutronic environment in three dimensions, and calculates the changed flow area, wetted perimeters, gaps between the fuel pins and distances between the outermost pins and the wrapper tube wall. It also calculates magnitudes, positions and directions of the contact forces loaded by the adjacent fuel pins or wrapper tube. Relative deflections of fuel pins modifies the initial nominal geometry of coolant flow channels, and associated temperature distributions in the flow channels accordingly. For this reason, the changed geometry of the coolant flow channels calculated by SHADOW is fed back to the thermal-hydraulic analysis code again to reevaluate the modified temperature distribution.

#### 4. Analysis of Deformation of 169 Fuel Pins due to Thermal Bowing

A fuel assembly of a prototype sodium-cooled fast breeder reactor has been treated by SHADOW for analyzing the deformation of fuel pins due to thermal bowing. The assembly contains 169 fuel pins, and its cross-sectional view is shown in Fig. 6, which also clarifies fuel pin identifiers. The major geometrical data of the fuel assembly components are given in Table I and Fig. 7.

Fig. 8 shows radial temperature distributions of the coolant within the fuel assembly, which were calculated by the thermal-hydraulic analysis code DIANA. Coolant flow channel number is shown in Fig. 9. The fuel pins numbered by 128 and 149 have the maximum and the minimum powers in the assembly, respectively, and the ratio between these values is 1.42. The radial temperature gradient reaches its maximum in the Y direction and the temperature distribution is almost symmetric with respect to the Y axis.

The axial shape of deformed fuel pins within the straight standing wrapper tube is shown in Fig. 10, which represent the component of fuel pin displacement in the Y direction. The fuel pins displace to the left side except for the upper part of the gas plenum section, which is attributable to the temperature gradient towards the Y direction. From this figure, it can be seen that the bowing deformation is significant throughout the entire length of the outer fuel pins and in the upper part of the gas plenum section of the inner ones.

Fig. 10 also shows the contact points along the Y axis either between the adjacent fuel pins or between the fuel pin and the wrapper tube wall. The contact forces are all applied to the fuel pins through the wire spacer except for the top of the outermost fuel pins. The major contact forces are loaded on the top of the outer fuel pin and on the center port of the gas plenum and core sections of the inner fuel pin.

Fig. 11 shows the axial (Z-directional) variation of the coolant flow channel areas on the Y axis, where the cross-sectional area of the wire spacer is not taken into account. In the inner flow channel, the flow area varies little from its nominal value except for the upper part of the gas plenum section, whereas that of the outer flow channel reduces from its nominal value by 17% in the heat-generated section.

The deformed coolant flow channels change the temperature distribution of coolant in the fuel assembly as shown in Fig. 12. The maximum temperature in the deformed channels is almost the same as in the undeformed nominal channels, and its position shifts into the inner region of the fuel assembly, which results in the flatter temperature distribution in the inner region. The large increase of coolant temperature in the outer channel 294 is due to the decrease of the channel areas in the heat-generated section. These changes of temperature distribution can cause the further deformation of the fuel pins, which requires iterative estimations of the temperature distribution in the deformed channels.



## 5. Conclusion

A new analytical method has been presented for three-dimensional analysis of the mechanical response of fuel pins with wire spacers, to their thermal and neutronic environment in an assembly of a LMFBFR.

Based on this method, a computational code, SHADOW, has been developed, which can be applied to seven kinds of wire wrap fuel assemblies with the number of fuel pins ranging from 7 to 169.

A fuel assembly of a prototype fast breeder reactor was treated by SHADOW for analyzing the deformation of 169 fuel pins due to thermal bowing. Conclusions derived from the present study are summarized as follows.

- (1) The bowing deformations are significant throughout the overall length of the outer fuel pins and in the upper part of the gas plenum section of the inner fuel pins. These phenomena cause the axial variations of the coolant flow areas, especially, in the outer channels.
- (2) The deformation of coolant flow channels has little effect on the maximum coolant temperature, but makes the hot spot move into the inner region of the assembly. The change of temperature distribution can cause the further deformation of fuel pins, which requires iterative estimations of the temperature distribution in the deformed channels.
- (3) In the case of the outer fuel pins, the major contact forces are loaded near the top of each fuel pin, and in the case of the inner ones, the loads are mainly applied near the center parts of the gas plenum and core sections. These forces are not large enough to deform the cross section of the cladding.

## ACKNOWLEDGEMENT

The author would like to acknowledge Mr. R. Takeda, Dr. K. Inoue and Mr. T. Konishi of the Atomic Energy Research Laboratory, Hitachi Ltd., for their valuable discussions, and to Dr. K. Taniguchi and Dr. S. Kobayashi for their sustained encouragement. Acknowledgement is also due to Mr. S. Hirao and Mr. H. Hayashi of Hitachi Works, Hitachi Ltd., for providing the author with technological information for this study.

## REFERENCES

- [1] OHMAE, K., MORINO, A., NAKAO, N., HIRAO, S., "Channel Deformation Analysis for Fast Reactor Fuel Assemblies Undergoing Swelling and Thermal Bowing", Nucl. Eng. Design 23, 309-320 (1972).
- [2] EICKHOFF, K.G., "Theoretical and Experimental Studies Supporting the Design of Fast Reactor Fuel Elements", Proc. Symp. on Fuel and Fuel Elements for Fast Reactors, IAEA-SM-173/61 (1974).

- [3] McAREAVEY, G., "Thermal Bowing of Pins in Fuel Element Clusters", Proc. the Third Intl. Conf. on Structural Mechanics in Reactor Technology, London, England, (1975).
- [4] BAUMGARTNAR, A.J., "Response of a Tightly Clustered Nuclear Fuel Element Bundle to Arbitrary Initial Thermal and Mechanical Loading Conditions", Proc. the First Intl. Conf. on Structural Mechanics in Reactor Technology, Berlin, Germany, (1971).
- [5] OHMAE, K., OHTSUKI, A., KANETO, K., "Fast Reactor Core Deformation due to Stainless Steel Swelling and Thermal Bowing with Irradiation Enhanced and Thermal Creep", Nucl. Eng. Design 23, 86-106 (1972).
- [6] HIRAO, S., NAKAO, N., "DIANA - A Fast and High Capacity Computer Code for Interchannel Coolant Mixing in Rod Arrays", Nucl. Eng. Design 30, 214-222 (1974).
- [7] FOWLER, T.B., VONDY, D.R., "Nuclear Reactor Core Analysis Code: CITATION", ORNL - TM - 2496, Rev. 1, Jan. (1970).

Table I Geometrical Data of Fuel Assembly Components

Fuel pin length	281 cm
Fuel pin diameter	0.65 cm
Cladding thickness	0.047 cm
Wire spacer diameter (inner/outer-most)	0.137/0.09 cm
Wire spacer pitch (P)*	30.8 cm
Wire spacer initial axial position (L)*	1.2 cm
Wire spacer initial and final angular positions from the reference direction ( $\theta_1, \theta_2$ )*	190°
Orientation of wrapping*	Counterclockwise, viewed from above the fuel pin
Fuel pin pitch	0.793 cm
Wrapper tube length	360 cm
Wrapper tube inner wall flat-to-flat distance	10.46 cm
Distance between the knock-bar (lower end of a fuel pin) and upper support plate of an assembly	50.5 cm

\* Refer to Fig. 7.

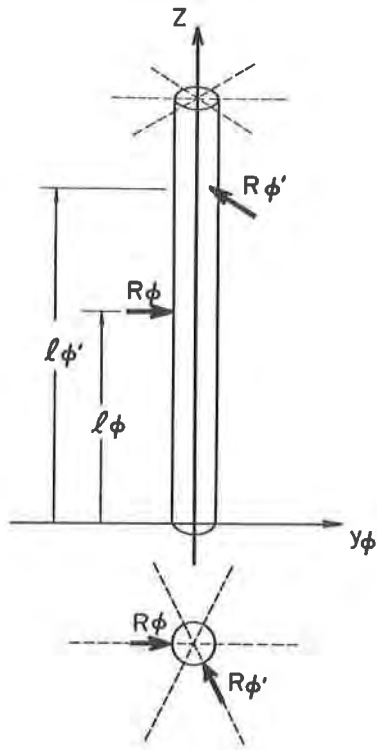


Fig. 1 Model of a Fuel Pin Loaded by Contact Forces

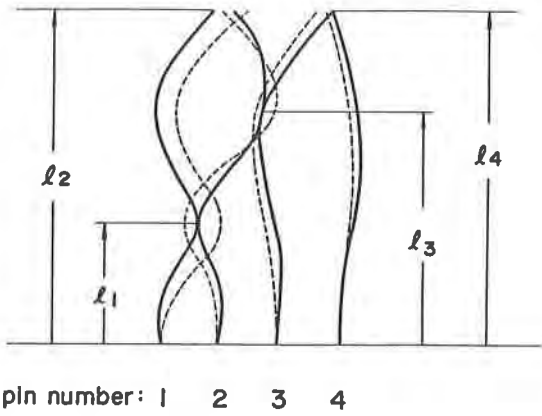


Fig. 2 Axial Height of Contact Points on the Fuel Pins

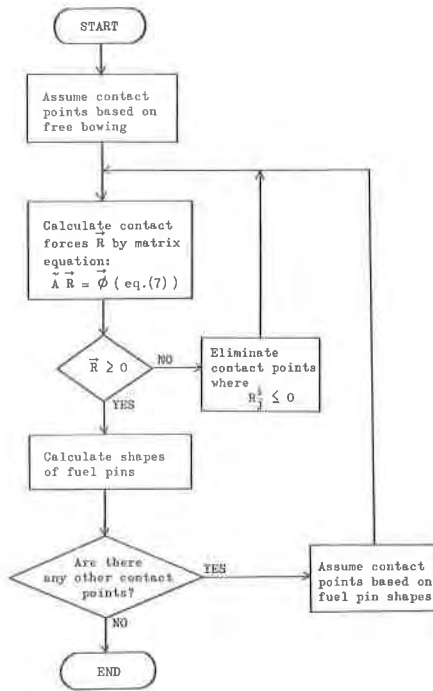


Fig. 3 Flow Chart for Locating Contact Points on the Fuel Pins

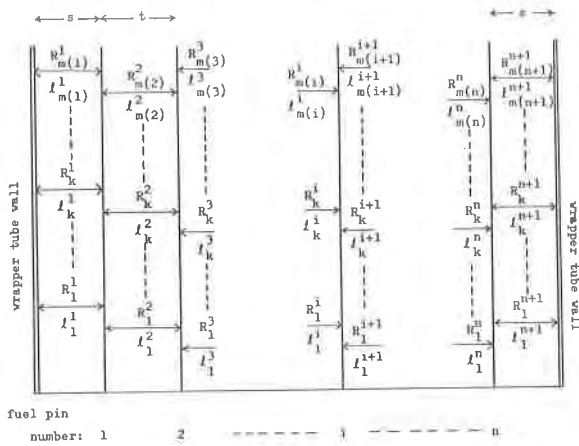


Fig. 4 Contact Force,  $R_j^i$ , and Axial Height of Contact Point,  $l_j^i$ , on the Fuel Pins in a Row

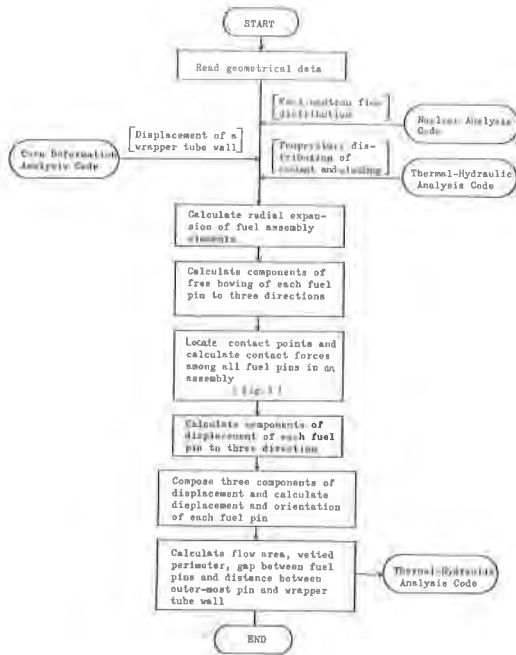


Fig. 5 Calculational Steps in SHADOW

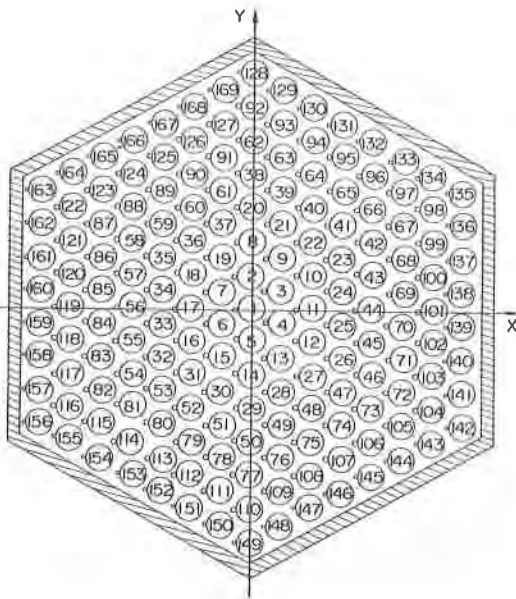


Fig. 6 Cross-sectional View of the Assembly with Fuel Pin Identifiers Used in the Study

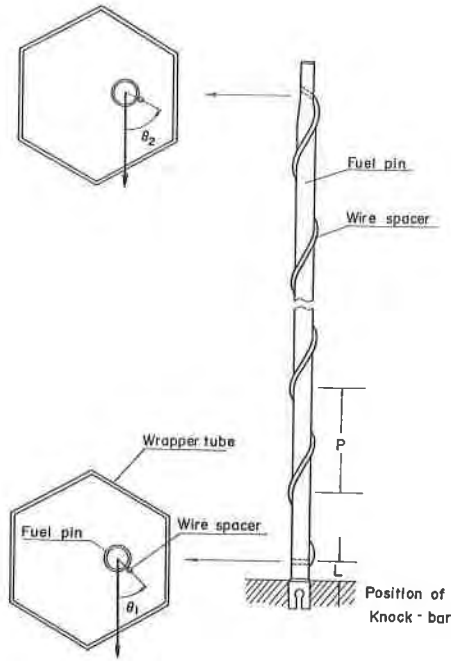


Fig. 7 Configurations of Fuel Pin with Wire Spacer and its Cross Section in a Wrapper Tube

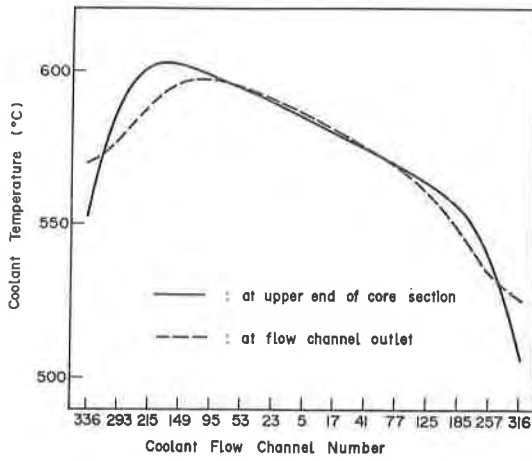


Fig. 8 Radial Distribution of Coolant Temperature

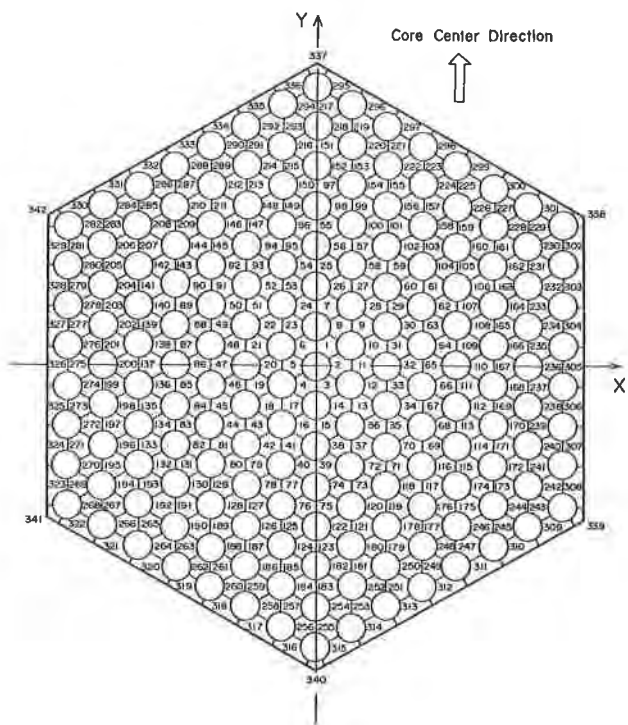


Fig. 9 Coolant Flow Channel Number

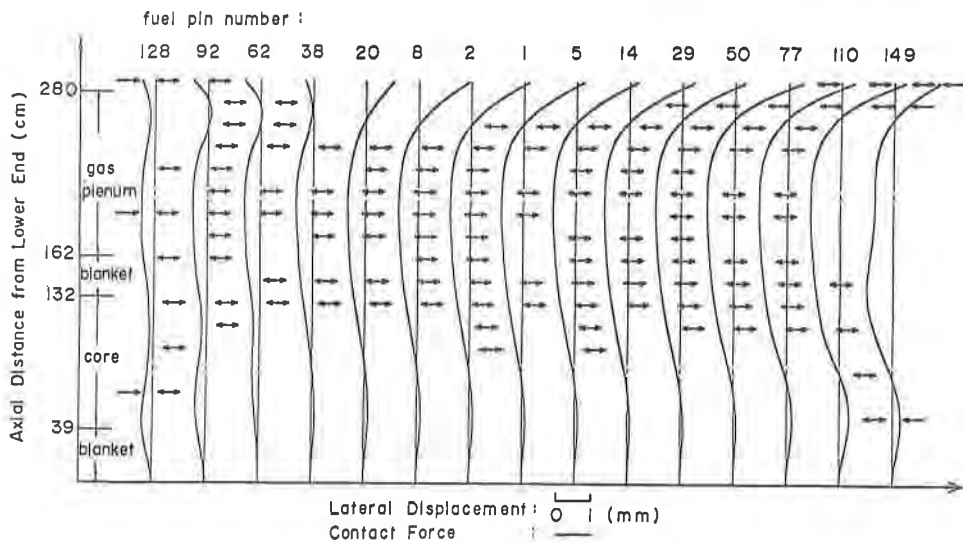


Fig. 10 Displacements of Fuel Pins in a Row and Contact Forces

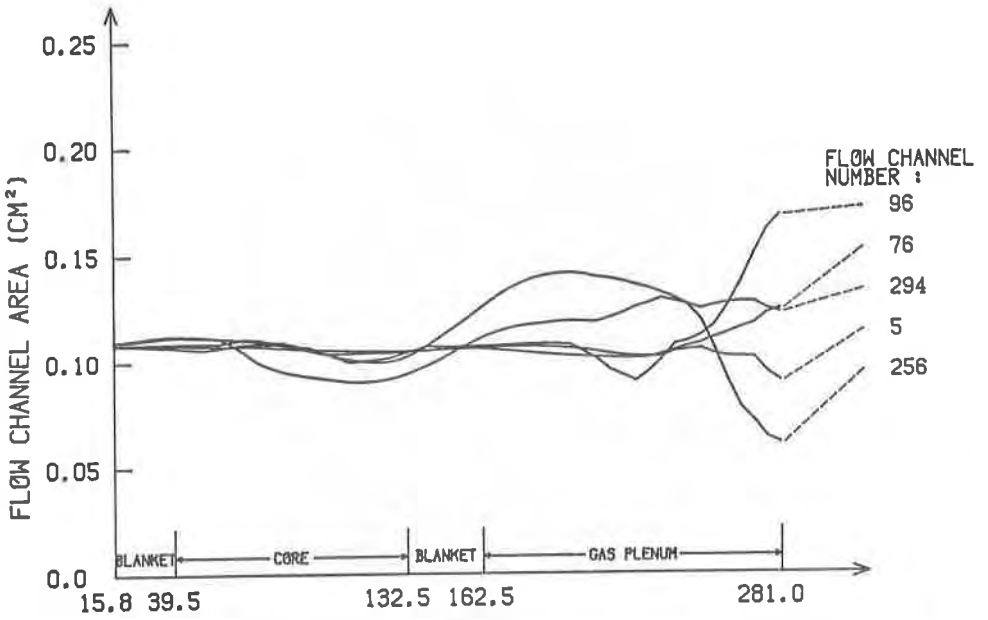


Fig. 11 Axial Change of Flow Channel Area

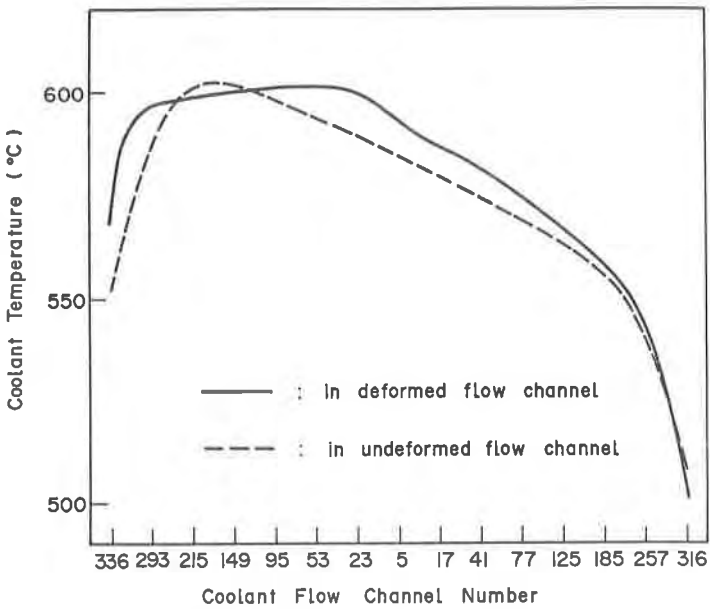


Fig. 12 Radial Distribution of Coolant Temperature in Deformed Flow Channel (at Upper End of Core Section)